A Census of Plane Graphs with Polyline Edges*

Andrea Francke† Csaba D. Tóth‡

Abstract

We study vertex-labeled graphs that can be embedded on a given point set such that every edge is a polyline with k bends per edge, where $k \in \mathbb{N}$. It is shown that on every n-element point set in the plane, at most $\exp(O(n \log(2+k)))$ labeled graphs can be embedded using polyline edges with k bends per edge, and this bound is the best possible. This is the first exponential upper bound for the number of labeled plane graphs where the edges are polylines of constant complexity. Standard tools developed for the enumeration of straight-line graphs, such as triangulations and crossing numbers, do not seem applicable in this scenario. Furthermore, the exponential upper bound does not carry over to other popular relaxations of straight-line edges: for example, the number of labeled planar graphs that admit an embedding with x-monotone edges on n points is super-exponential.

1 Introduction

A *plane graph* is an abstract graph $G = (V, E)$ together with an embedding into the Euclidean plane that maps the vertices in V to distinct points in $\mathbb{R}^2$, and maps the edges in E to Jordan arcs between the corresponding vertices such that any two arcs can intersect only at a common endpoint. A *plane straight-line graph* is a plane graph where the edges are mapped to straight-line segments.

Determining the number of (labeled) plane straight-line graphs that can be embedded on a finite vertex set $V \subset \mathbb{R}^2$ has received continued attention, motivated by randomized algorithms on the configuration space of such graphs. Ajtai et al. [2] proved that every set of n points in the plane admits at most $O(c^n)$ plane straight-line graphs for some absolute constant $c < 10^{13}$. This upper bound has successively been improved over the last decades: the current best upper bound $O(187.53^n)$ is due to Sharir and Sheffer [32], using a so-called cross-graph charging scheme [30, 33]. The current best lower bound, $\Omega(41.18^n)$, is due to Aichholzer et al. [1]. The quest for finding the maximum number of plane straight-line graphs and other common graphs (such as triangulations, Hamilton cycles, and matchings) continues with the search for extremal configurations and efficient algorithms for given point sets [3]. All results in this area rely on the simple fact that a plane straight-line graph contains at most one diagonal for any four points in convex position (Fig. 1). This fact is a crucial ingredient of (i) the celebrated Crossing Lemma by Ajtai et al. [2], (ii) the notion of *edge flips* in geometric triangulations [24], and also (iii) the cross-graph charging scheme in [30, 33].

In this paper, we study the maximum number of graphs on n (labeled) vertices that admit a plane embedding on n given points with polyline edges with k bends per edge for $k > 0$. An *edge with k bends* (or *k-bend edge*, for short) is a polyline that consists of $k+1$ line segments. For a set S of n points in Euclidean plane, and an integer $k \geq 0$, we denote by $B_k(S)$ the family of (labeled) graphs that admit a plane embedding with k-bend edges such that the vertices are mapped onto S. We may identify the labeled vertices with the corresponding points in the plane, and denote a graph $G \in B_k(S)$ by $G = (S, E)$. For example, $G \in B_0(S)$ if it is a planar straight-line graph on the vertex set S.

*A preliminary version of this paper has appeared in the *Proceedings of the 30th Symposium on Computational Geometry*, pages 242–250, ACM Press, 2014.

†Institute of Theoretical Computer Science, ETH Zürich, CH-8092 Zürich, Switzerland.
Current affiliation: Google Inc., Zürich, Switzerland. andrea.francke@gmail.com

‡California State University Northridge, Los Angeles, CA, USA. cdtoth@acm.org

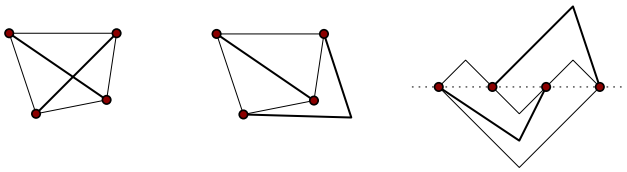

Figure 1: Left: the diagonals of a convex quadrilateral cross. Middle: both diagonals can be realized with polylines with (at most) one bend per edge. Right: K_4 on four collinear points can be embedded with polylines with one bend per edge.

For $n, k \in \mathbb{N}$, let $b_k(n) = \max_{|S|=n} |B_k(S)|$, that is, the maximum cardinality of $B_k(S)$ over all n-element point sets S. The main result of the paper is the following.

Theorem 1 *There is an absolute constant $c > 0$ such that $b_k(n) \le 2^{cn\log(2+k)}$ for all $k, n \in \mathbb{N}$.*

Previously, an exponential upper bound was known only in the case $k = 0$ (cf. [2, 32]). Pach and Wenger [29] showed that *every* n-vertex (labeled) planar graph embeds on every n-element point set with at most $120n$ bends per edge. They also constructed (labeled) planar graphs and point sets such that any plane embedding with polyline edges requires at least $\Omega(n^2)$ bends in total. Thus their bound on the total number of bends is the best possible apart from constant factors. The number of planar graphs on n labeled vertices is known to be $\Theta(n^{-7/2}\gamma^n \cdot n!)$, where $\gamma \approx 22.27$ [21]. Combined with [29], this implies that the number of n-vertex labeled graphs that embed on an n-element point set with $120n$-bend edges is $2^{O(n\log n)}$. Theorem 1 improves on this bound when $k = o(n)$.

The following simple construction shows that Theorem 1 is the best possible, apart from the constant c. Assume that $n \ge k \ge 122$. Given a set S of n points in the plane, partition the plane by parallel lines into strips, each containing $n' = \lfloor k/122 \rfloor$ points with the possible exception of one strip. In each strip, independently, all planar graphs can be realized with at most $120+2$ bends per edge, using the result of Pach and Wenger [29], but truncating the edges at their first and last intersection points (if any) with the parallel lines on the boundary of the strips. The number of planar graphs on n' vertices is $2^{\Theta(n'\log n')} = 2^{\Theta(k\log k)}$. Combining the graphs in $\lfloor n/n' \rfloor = \Theta(n/k)$ strips, each containing n' points, we obtain $\left(2^{\Theta(k\log k)}\right)^{n/k} = 2^{\Theta(n\log k)}$ labeled planar graphs.

Generalizations. Our proof for Theorem 1 extends to a more general setting: we can formulate it in terms of the total number of bends, and in terms of topological equivalence classes of plane graphs. Let $G_0 = (S, E_0)$ and $G_1 = (S, E_1)$ be two plane graphs on the same vertex set $S \subset \mathbb{R}^2$ such that the corresponding abstract graphs are isomorphic (but the embedding of the edges may be different). The plane graphs G_0 and G_1 are *isotopic* if there is a continuous family of plane graphs $(G_t)_{t\in[0,1]}$ between G_0 and G_1 (where the edges are deformed continuously and remain interior-disjoint). Equivalently, G_0 and G_1 are isotopic if they have the same outer face and the same rotation system (that is, the counterclockwise orders of incident edges are the same at each vertex); see [23]. Isotopy is an equivalence relation on the plane graphs on the vertex set S. For $K \in \mathbb{N}$, let $T_K(S)$ denote the set of isotopy classes of plane graphs on S that have polyline edges with a total of at most K bends. For example, $T_0(S)$ is the set of isotopy classes of planar straight-line graphs on S.

For $n, K \in \mathbb{N}$, let $t_n(K) = \max_{|S|=n} |T_K(S)|$, that is, the maximum cardinality of $T_K(S)$ over all n-element point sets S. We prove the following generalization of Theorem 1.

Theorem 2 *There is an absolute constant $c > 0$ such that $t_K(n) \le 2^{cn\log(2+K/n)}$ for all $K, n \in \mathbb{N}$.*

Comparison to the Unlabeled Setting. If we are interested in the number of unlabeled graphs that embed into a given point set using polyline edges, we have quite a different picture. In this case, a vertex of graph G may be mapped to any point in S. Kaufmann and Wiese [25] proved that *every* n-vertex planar graph admits an embedding into *every* set of n points in the plane with 2-bend edges. Everett et al. [20] constructed an n-element point set S_n such that *every* n-vertex planar graph admits an embedding into S_n with 1-bend edges. In both cases, we cannot choose arbitrarily which vertex is mapped to which point. Note, however, that the number of pairwise nonisomorphic n-vertex planar graphs is only singly-exponential in n: Turán [35] gave an upper bound of 2^{12n} based on succinct representations of planar graphs, which was later improved to $2^{4.91n}$ [8]. Hence, the results in [20, 25] yield only an exponential lower bound (and no upper bound) for the number of *labeled* graphs that embed on n points with 1- or 2-bend edges, respectively.

Triangulations. Triangulations play a crucial role in counting plane straight-line graphs: for example, bounds for Hamilton cycles and spanning trees on a point set have been derived from the number of triangulations (by finding subgraphs of a triangulation, ignoring the location of the vertices). This partly justifies the continued interest in triangulations on point sets [1, 16, 31]. We show that this important tool is unavailable when dealing with plane graphs embedded with polyline edges, since edge-maximal graphs exist in $B_1(S)$ that are not subgraphs of triangulations.

A *combinatorial triangulation* is an edge-maximal planar graph. By Euler's formula, if $G = (V, E)$ is a combinatorial triangulation, then $|E| = 3|V| - 6$ for $|V| \geq 3$; and every face in a plane embedding of G is bounded by precisely three edges. A *geometric triangulation* is an edge-maximal planar straight-line graph (that is, no new edges can be added to the given straight-line embedding); here all bounded faces are triangles, and the outer face is the complement of the convex hull of S. That is, in an edge-maximal graph in $B_0(S)$, all bounded faces are triangles. We show that the bounded faces of an edge-maximal graph in $B_1(S)$ are not necessarily triangles.

Theorem 3 *For every $f, h \in \mathbb{N}$, with $f \geq 4$ and $h \geq 1$, there is a point set S and a graph $G = (S, E)$ such that G is an edge-maximal graph in $B_1(S)$ and every 1-bend plane embedding of G has at least h bounded faces each with f edges.*

Monotone embeddings. Theorem 1 gives an upper bound on the number of n-vertex labeled planar graphs that admit an embedding on n points in the plane if the edges are restricted to polylines with at most k interior vertices (bends). Can we derive a similar result if we allow Jordan arcs with some other combinatorial or geometric restrictions? The proof of Theorem 1 is likely to go through if replace the straight-line segments in the polylines by convex arcs (a arc in $\mathbb{R}^2$ is called *convex* if it lies on the boundary of a convex body). A possible further relaxation would replace the straight-line segments by monotone arcs, but in this case, we can show that the exponential upper bound does not hold anymore.

A *monotone plane graph* is a plane graph where every edge is embedded as an x-monotone Jordan arc. It is a popular generalization of planar straight-line graphs. However, the number of labeled graphs that admit a monotone plane embedding on a given point set is already super-exponential. Note that every monotone plane graph can be triangulated (i.e., every face with 4 or more vertices can be subdivided by an x-monotone diagonal), as shown by Pach and G. Tóth [28].

Theorem 4 *For every set S of n points in the plane, no two on a vertical line, at least $\lfloor (n-2)/2 \rfloor !$ labeled planar graphs with $n \geq 4$ vertices admit a monotone embedding on S.*

Recently, Angelini et al. [4] considered *bimonotone* drawings, where each edge is embedded as an x- and y-monotone Jordan arc. They classify plane graphs that admit such an embedding, and show that if the embedding is possible, then one bend per edge suffices.

Organization. We review useful tools from computational topology on homotopic shortest path with respect to a discrete point set S in the plane in Section 2. We prove Theorems 1 and 2 in Section 3, using an efficient combinatorial representation of homotopic shortest paths. We construct plane graphs with polyline edges that cannot be triangulated using polylines of the same number of bends in Section 4; and we consider monotone plane graphs in Section 5. We conclude in Section 6 with a few open problems.

2 Preliminaries

The proof of Theorem 1 is based on a reduction to plane *straight-line* graphs. Given a plane graph $G = (S, E)$ with k bends per edge, we replace each edge with a homotopic shortest path. The union of the shortest paths forms a plane straight-line graph $G' = (S, E')$ on S. Note that the shortest paths may overlap, and the same straight-line graph G' may be obtained in this way from several k-bend plane graphs on S. Theorem 1 follows from an $2^{O(n)}$ bound on the number of plane straight-line graphs $G = (S, E')$ [32], combined with an $2^{O(n \log(2+k))}$ bound on the number of k-bend plane graphs that correspond to a common straight-line graph $G' = (S, E')$. The latter bound is obtained by encoding the shortest paths homotopic to the k-bend edges of G with $O(n \log(2 + k))$ bits of information.

Efficient encodings of various combinatorial structures have been studied for decades in the context of *succinct representation*. Bereg [7] showed that the family of (possibly crossing) simple k-bend polylines between the same two points (i.e., parallel edges) among n points in the plane can be *encoded* by a weighted complete graph K_n on the point set, where the weight of each edge is the number of times the homotopic shortest paths traverse that edge. He shows that $O(n \log(n+k))$ bits of information suffice for the encoding; and this bound is the best possible for $k = \Omega(n^{1+\varepsilon})$ for all $\varepsilon > 0$. Theorem 1 offers a better bound when the polylines may have different endpoints but are pairwise noncrossing (i.e., they are edges of a plane graph) and $k = o(n)$. The main technical difficulty is to encode pairwise noncrossing polylines efficiently. For 1-bend embeddings, we use combinatorial properties of homotopic shortest paths; and for $k \geq 2$, we reduce k-bend graphs to 1-bend graphs.

Let us note that the following naïve idea for a direct reduction to plane straight-line graphs does not yield any reasonable bound. Given a plane graph $G = (S, E)$ with k-bend edges, we could introduce new vertices at each bend point, and obtain a plane straight-line graph on at most $n + (3n - 6)k = O(kn)$ vertices. Any set of $m = O(kn)$ points in the plane admits $O(187.53^m) = 2^{O(kn)}$ plane straight-line graphs [32]. This bound assumes that the set of bend points is fixed. However, each bend point can be positioned at $\Theta(m^4)$ combinatorially different locations relative to m points in the plane in general position (the $\binom{m}{2}$ lines spanned by m points in general position form an arrangement with $\Theta(m^4)$ cells). Guessing successively the relative positions for $m = \Theta(kn)$ unlabeled bend points leads to $\frac{1}{m!} \prod_{i=0}^{m-1} \Theta((n + i)^4) = 2^{\Theta(kn \log n)}$ possibilities. Thus this approach gives an upper bound of $b_k(n) = 2^{O(kn \log n)}$, which is much worse than Theorem 1.

2.1 Geodesic Representation

An *arc* in Euclidean plane is a continuous function $\gamma : [0, 1] \to \mathbb{R}^2$; an arc is *simple* if γ is injective. Let S be a set of n points in the plane, no three of which are collinear (this assumption is not essential for the argument, and can be removed by standard tools, e.g., virtual perturbation). The set $\mathbb{R}^2 \setminus S$ is called the *punctured plane*. We denote by $\Gamma(S)$ the set of all arcs between distinct points in S, and by $\Gamma_0(S) \subset \Gamma(S)$ the set of arcs that do not pass through any point in S (i.e., $\gamma(t) \notin S$ for $0 < t < 1$). Two arcs $\gamma_1, \gamma_2 \in \Gamma(S)$ between the same two points $s_1, s_2 \in S$ are *homotopic* (with respect to S) if there is a continuous function $f : [0, 1]^2 \to \mathbb{R}^2$ such that no interior point in $(0, 1)^2$ is mapped to any point in S, and on the boundary of $[0, 1]^2$, we have $f(0, t) = \gamma_1(t)$, $f(1, t) = \gamma_2(t)$, $f(t, 0) = s_1$, and $f(t, 1) = s_2$ for all $t \in [0, 1]$. Intuitively, γ_1 can be continuously deformed into γ_2 such that the two endpoints remain fixed, and the intermediate arcs are do not pass through any point in S (however, γ_1 or γ_2 may pass through points in S). Note that

homotopy is an equivalence relation over $\Gamma_0(S)$; but it is not transitive over $\Gamma(S)$. For an arc $\gamma \in \Gamma_0(S)$, let $\hat{\gamma} \in \Gamma(S)$ be the shortest arc homotopic to γ.

Finding the shortest arc homotopic to a given polyline with respect to a point set S has been studied intensely. Hershberger and Snoeyink [22] gave an efficient algorithm for computing $\hat{\gamma}$ for a given simple polyline γ. Efrat et al. [18] show how to compute $\hat{\gamma}$ for all γ in a set of polygonal arcs with distinct endpoints simultaneously. Later Bereg [6] improved the runtime of this algorithm: for a family of pairwise disjoint simple polylines, the runtime is $O(n \log^{1+\varepsilon} n + k_{\text{in}} \log n + k_{\text{out}})$ for any fixed $\varepsilon > 0$, where k_{in} and k_{out} are the total number of edges of the input and output arcs, respectively. Colin de Verdière [11, 14] extended these techniques to pairwise interior-disjoint polylines, which may share endpoints, including a polyline embedding of a graph. Generalizations to nonsimple arcs and to surfaces of higher genus have also been studied (see [12, 13, 19] and the references therein).

Basic properties of shortest paths. For a plane graph $G = (S, E)$ with polyline edges, let $\widehat{E} = \{\hat{e} : e \in E\}$ be a set of homotopic shortest arcs for all edges in E. We briefly review well-known properties of homotopic shortest paths. If γ is a simple arc in the plane, then $\hat{\gamma}$ is a polyline with all interior vertices (i.e., bend points) in S. The path $\hat{\gamma}$ need not be a simple path: it may have repeated vertices. However, $\hat{\gamma}$ is *weakly simple* in the sense that for every $\varepsilon > 0$, the interior vertices of all shortest paths can be perturbed by at most ε to obtain a *simple* path in $\Gamma_0(S)$ that is homotopic to γ. (See also [10] for an equivalent definition in terms of the Fréchet distance). In particular, this implies that the path $\hat{\gamma}$ has no self-crossings.

Furthermore, for every $\varepsilon > 0$ the interior vertices of all shortest paths in $\widehat{E}$ can be simultaneously perturbed by at most ε to obtain a plane graph on S that is isotopic to G [11]. In particular, no two arcs in $\widehat{E}$ cross each other; see Fig. 2(a) and (c) for an example.

Angles of shortest paths. An *angular domain* (for short, *angle* or *wedge*) $\angle(a, b, c)$ is the set of points swept when we rotate the ray $\overrightarrow{ba}$ to $\overrightarrow{bc}$ counterclockwise about b. Two angles with the same apex, $\angle(a_1, b, c_1)$ and $\angle(a_2, b, c_2)$, are called *nested* if one contains the other. A vertex $s \in S$ in a plane straight-line graph on S is called *pointed* if all edges incident to s lie in a closed halfplane bounded by a line through s.

Consider a shortest path $\hat{\gamma} \in \widehat{E}$, $\hat{\gamma} = (s_1, \ldots, s_m)$, with possible repeated vertices. At each interior vertex s_i, $1 < i < m$, the two incident edges determine two angles: $\angle(s_{i-1}, s_i, s_{i+1})$ and $\angle(s_{i+1}, s_i, s_{i-1})$. One of them is convex and the other is reflex since no three points in S are collinear. Vertices s_1 and s_m are each incident to an *endsegment* of $\hat{\gamma}$.

Lemma 5 *At every $s \in S$, the convex angles of the shortest paths through s are nested, and they all contain the endsegments of the shortest paths incident to s.*

Proof. We use a common perturbation of the shortest paths in $\widehat{E}$ to homotopic simple paths [11]. For the first claim, let (a_{i-1}, a_i, a_{i+1}) and (b_{j-1}, b_j, b_{j+1}) be contained in some shortest paths in $\widehat{E}$ such that $s = a_i = b_j$, and both $\angle(a_{i-1}, a_i, a_{i+1})$ and $\angle(b_{j-1}, b_j, b_{j+1})$ are convex. We need to show that the angular domains $\angle(a_{i-1}, a_i, a_{i+1})$ and $\angle(b_{j-1}, b_j, b_{j+1})$ are nested.

Let d be the minimum distance between any point in S and a line passing through two other points in S; and let $\varepsilon = d/(2n)$. An ε-perturbation of $\widehat{E}$ contains two noncrossing paths $(\tilde{a}_{i-1}, \tilde{a}_i, \tilde{a}_{i+1})$ and $(\tilde{b}_{j-1}, \tilde{b}_j, \tilde{b}_{j+1})$, where the points $\tilde{a}_{i-1}$, $\tilde{a}_i$, $\tilde{a}_{i+1}$, $\tilde{b}_{j-1}$, $\tilde{b}_j$, and $\tilde{b}_{j+1}$ are each within distance ε from a_{i-1}, a_i, a_{j+1}, b_{j-1}, b_j, and b_{j+1}. The perturbed angles $\angle(\tilde{a}_{i-1}, \tilde{a}_i, \tilde{a}_{i+1})$ and $\angle(\tilde{b}_{j-1}, \tilde{b}_j, \tilde{b}_{j+1})$ are convex due to the choice of ε. Point $s = a_i = b_j$ lies in the interior of both convex angles, otherwise the path (a_{i-1}, a_i, a_{i+1}) or (b_{j-1}, b_j, b_{j+1}) could be replaced by a shorter homotopic path. Consequently, one of $\angle(a_{i-1}, a_i, a_{i+1})$ and $\angle(b_{j-1}, b_j, b_{j+1})$ contains the other.

For the second claim, let (a_1, a_2) be an endsegment of a path in $\widehat{E}$, and let (b_{j-1}, b_j, b_{j+1}) be part of some shortest path in $\widehat{E}$ such that $s = a_1 = b_j$, and $\angle(b_{j-1}, b_j, b_{j+1})$ is convex. In an ε-perturbation, point s lies

in the interior of $\angle(\tilde{b}_{j-1}, \tilde{b}_j, \tilde{b}_{j+1})$, and the path $(\tilde{b}_{j-1}, \tilde{b}_j, \tilde{b}_{j+1})$ is disjoint from $(a_1, \tilde{a}_2)$. Since the paths are noncrossing, the angular domain $\angle(b_{j-1}, b_j, b_{j+1})$ contains the endsegment a_1a_2. □

Corollary 6 *If $s \in S$ is an interior vertex of $\hat{e}$, for some $e \in E$, then s is pointed in $G' = (S, E')$.*

2.2 Encoding Homotopic Shortest Paths

In this section, we define two combinatorial representations of the homotopic shortest paths $\widehat{E}$, and a corresponding routing diagram isotopic to G, for a plane graph $G = (S, E)$.

Image Graph and Routing Diagram. Consider a plane graph $G = (S, E)$. Let E' be the union of all edges of the shortest paths in $\widehat{E} = \{\hat{e} : e \in E\}$. We define the *image graph* of G to be $G' = (S, E')$. By construction, G' is a plane straight-line graph on the vertex set S; see Fig. 2(a-b) for an example. Each shortest path in $\widehat{E}$ is a path in the image graph G', but not necessarily a simple path.

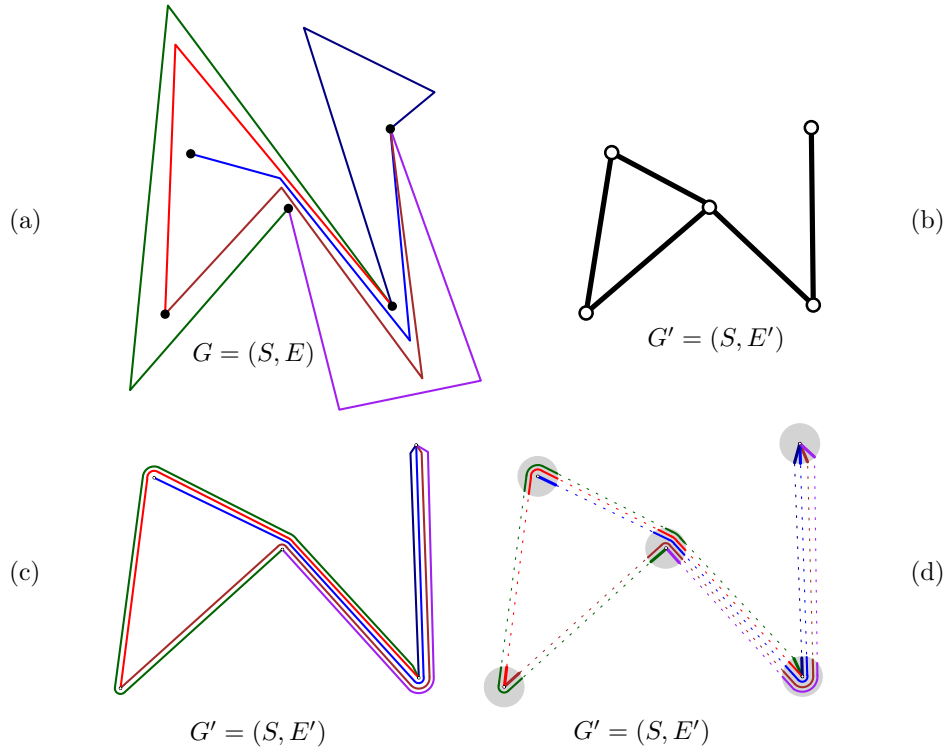

Figure 2: (a) A plane graph $G = (S, E)$ with 2-bend edges. (b) The graph $G' = (S, E')$ of the shortest homotopic paths. (c) The shortest homotopic paths are perturbed into interior-disjoint arcs in a routing diagram. (d) The signature of a routing diagram is uniquely determined by the local topology in the disks D_s.

For every $\varepsilon > 0$, the *ε-strip-system* of the image graph $G' = (S, E')$ consists of the following regions:

- For every point $s \in S$, let D_s be a disk of radius ε centered at s.
- For every edge $st \in E'$, let the *corridor* N_{st} be the set of points at distance at most ε^2 from the line segment st, outside of the disks D_s and D_t.

Denote by U_ε the union of all these disks and corridors. Let $\varepsilon > 0$ be sufficiently small such that the disks D_s are pairwise disjoint, the corridors $N(uv)$ are pairwise disjoint, and every corridor N_{st} of a segment intersects only the disks at its endpoints D_s and D_t.

A *routing diagram* (Fig. 2(c)) is a simultaneous perturbation of the edges in $\widehat{E}$ into a plane graph isotopic to $G = (S, E)$ such that every shortest path $\hat{e} = (s_1, \ldots, s_m)$ is replaced by a polygonal path in the ε-strip-system U_ε, that contains precisely one line segment in every disk D_{s_i}, $i = 1, \ldots, m$, and every corridor $N_{s_i s_{i+1}}$, $i = 1, \ldots, m-1$. Similar concepts have previously been used in [10, 15, 17, 27].

2.3 Cross-Metric Representation

Let $G = (S, E)$ be a plane graph with polyline edges, $e \in E$, and $\hat{e} = (s_1, \ldots, s_m)$. The polylines e and $\hat{e}$ may cross several times. We show how to decompose e and $\hat{e}$ into noncrossing homotopic subpaths, which will be used in Section 3.2.

We rely on a combinatorial representation of the arcs in $\Gamma_0(S)$, the so-called *cross-metric surface model* [11, 12]. Let $T = (S, E'')$ be an arbitrary triangulation of the image graph G', together with a ray r_0 (an "infinite edge") from the leftmost vertex $s_0 \in S$ to infinity parallel to the negative x-axis. Then all faces of T are simply connected: the bounded faces are triangles, and the ray r_0 makes the outer face simply connected, as well. We direct all edges of T arbitrarily. Consider an arc $\gamma \in \Gamma_0(S)$ that crosses the edges of T transversely. The sequence of edges of T crossed by γ defines a *word* $w(\gamma)$ over the alphabet $\{a, a^{-1} : a \in E''\}$. Specifically, if γ crosses edge a of T from left to right (resp., right-to-left), the word $w(\gamma)$ contains a (resp, a^{-1}). Every letter in $w(\gamma)$ corresponds to an intersection point between γ and an edge of T.

For every arc $\gamma \in \Gamma_0(S)$ from s_1 to s_m, represented by a word $w(\gamma)$, one can easily compute the shortest word $\hat{w}(\gamma)$ of any other arc in $\Gamma_0(S)$ homotopic to γ by repeatedly applying the following operations:

1. delete any two adjacent letters aa^{-1} or $a^{-1}a$;
2. delete any first (resp., last) letter a or a^{-1} where edge a is incident to s_1 (resp., s_m).

Note, however, that for every edge $e \in E$, the homotopic shortest path $\hat{e}$ follows the edges of the image graph G', and so it does not cross any edge of T. Suppose $\hat{e} = (s_1, \ldots, s_m)$, and it is perturbed to a simple path $\tilde{e} = (\tilde{s}_1, \tilde{s}_2, \ldots, \tilde{s}_m) \in \Gamma_0(S)$ homotopic to e, where $\tilde{s}_1 = s_1$, $\tilde{s}_m = s_m$, and $\tilde{s}_i \in D_{s_i}$ for $1 < i < m$. Then the word corresponding to $\tilde{e}$ is $\hat{w}(e)$, that is $w(\tilde{e}) = \hat{w}(e)$. The following lemma characterizes all crossings between the shortest path $\hat{e}$ and its perturbation $\tilde{e}$. An interior edge $s_i s_{i+1}$, $2 \le i \le m-2$, is called an *inflection* edge of $\hat{e}$ if $\angle(s_{i-1}, s_i, s_{i+1}) < \pi < \angle(s_i, s_{i+1}, s_{i+2})$ or $\angle(s_{i-1}, s_i, s_{i+1}) > \pi > \angle(s_i, s_{i+1}, s_{i+2})$; see Fig. 3 for an example.

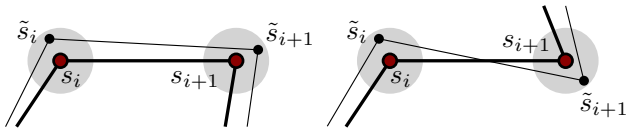

Figure 3: Left: Two consecutive convex angles $\angle(s_{i-1}, s_i, s_{i+1}) < \pi$ and $\angle(s_i, s_{i+1}, s_{i+2}) < \pi$. Right: An inflection edge $s_i s_{i+1}$ with $\angle(s_{i-1}, s_i, s_{i+1}) < \pi < \angle(s_i, s_{i+1}, s_{i+1})$.

Lemma 7 *Let $\hat{e} = (s_1, \ldots, s_m)$ and $\tilde{e} = (\tilde{s}_1, \tilde{s}_2, \ldots, \tilde{s}_m)$. The line segments $s_i s_{i+1}$ and $\tilde{s}_j \tilde{s}_{j+1}$ cross if and only if $i = j$ and $s_i s_{i+1}$ is an inflection edge of $\hat{e}$.*

Proof. First note that $s_1 s_2$ and $\tilde{s}_1 \tilde{s}_2$ do not cross since they have a common endpoint $s_1 = \tilde{s}_1$; similarly $s_{m-1} s_m$ and $\tilde{s}_{m-1} \tilde{s}_m$ do not cross. Since $\tilde{s}_j \tilde{s}_{j+1}$ lies in the ε-neighborhood of $s_j s_{j+1}$, it can possibly cross at most three segments: $s_{j-1} s_j$, $s_j s_{j+1}$, and $s_{j+1} s_{j+2}$. Recall that the angular domain $\angle(\tilde{s}_{i-1}, \tilde{s}_i, \tilde{s}_{i+1})$ contains s_i if and only if $\angle(s_{i-1}, s_i, s_{i+1}) < \pi$. Therefore, $\tilde{s}_j \tilde{s}_{j+1}$ crosses neither $s_{j-1} s_j$ nor $s_{j+1} s_{j+2}$; but it may cross $s_j s_{j+1}$.

If two consecutive angles are convex (that is, $\angle(s_{j-1}, s_j, s_{j+1}) < \pi$ and $\angle(s_j, s_{j+1}, s_{j+2}) < \pi$), then the intersection of the perturbed domains $\angle(\tilde{s}_{j-1}, \tilde{s}_j, \tilde{s}_{j+1}) \cap \angle(\tilde{s}_j, \tilde{s}_{j+1}, \tilde{s}_{j+2})$ contains both s_j and s_{j+1}, hence the entire segment $s_j s_{j+1}$. Consequently, $\tilde{s}_j \tilde{s}_{j+1}$ does not cross $s_j s_{j+1}$. Similarly, if two consecutive angles at s_j and s_{j+1} are reflex, then $\tilde{s}_j \tilde{s}_{j+1}$ does not cross $s_j s_{j+1}$. However, if $s_j s_{j+1}$ is an inflection edge, then the convex angular domains at $\tilde{s}_j$ and $\tilde{s}_{j+1}$ lie on opposite sides of the line through $\tilde{s}_j \tilde{s}_{j+1}$, and they contain points s_j and s_j, respectively. Consequently, segment $s_j s_{j+1}$ crosses $\tilde{s}_j \tilde{s}_{j+1}$, as claimed. □

By Lemma 7, every inflection edge of $\hat{e} = (s_1, \ldots, s_m)$ crosses the corresponding perturbed edge in $\tilde{e}$. Since $\tilde{e}$ and e are homotopic in $\Gamma_0(S)$, the arc e crosses every inflection edge of $\hat{e} = (s_1, \ldots, s_m)$.

Lemma 8 *Let $\hat{e} = (s_1, \ldots, s_m)$. Then there is a sequence of intersection points $X = (x_1, \ldots, x_\ell)$ in $e \cap \hat{e}$ such that $x_1 = s_1$, $x_\ell = s_m$, there is a point x_i on each inflection edge of $\hat{e}$, and the corresponding subarcs of e and $\hat{e}$ between consecutive points in X are interior-disjoint and homotopic.*

Proof. The word $w(e)$ can be reduced to the word $\hat{w}(e)$ by the two operations above, and $\hat{w}(e)$ corresponds to the perturbation $\tilde{e}$ of the shortest path $\hat{e}$. By Lemma 7, the paths $\hat{e}$ and $\tilde{e}$ cross once at each inflection edge. These intersection points correspond to letters in the word $\hat{w}(e)$, which in turn correspond to intersection points between e and $\hat{e}$. Let $(x_2, \ldots, x_{\ell-1})$ be the sequence of these intersection points in $e \cap \hat{e}$; and put $x_1 = s_1$ and $x_\ell = s_m$. Then, by construction, the subarcs of e and $\hat{e}$ between x_i and x_{i+1} are homotopic for $i = 1, \ldots, \ell - 1$. However, the subarcs of e and $\hat{e}$ between x_i and x_{i+1} may still cross each other, and we need to refine the subdivision induced by X.

While the subarcs of e and $\hat{e}$ between x_i and x_{i+1} intersect for some $i = 1, \ldots, \ell - 1$, we insert a new intersection point into X between x_i and x_{i+1} as follows. If the subarcs of e and $\hat{e}$ between x_i and x_{i+1} cross, then the crossing is recorded by some letter in the word $w(e)$ (since T is the triangulation of the image graph G'). Let a be the first such letter in $w(e)$, representing an intersection point $y \in e \cap \hat{e}$. Since $\tilde{e}$ and $\hat{e}$ do not cross between inflection edges (Lemma 7), this letter a was removed when $w(e)$ was reduced to $\hat{w}(e)$. Consequently, there is either a matching letter a^{-1} between x_i and x_{i+1} that canceled a; or letter a corresponds to an edge incident to s_1 or s_m. In both cases, the subarcs of e and $\hat{e}$ between x_i and y (resp., y and x_{i+1}) are homotopic. Hence, we can insert y into X between x_i and x_{i+1}.

The above while loop terminates, as e and $\hat{e}$ cross in finitely many points. When it does, the corresponding subarcs of e and $\hat{e}$ between consecutive points in X are interior-disjoint and homotopic, as required. □

3 Plane Graphs with k-Bend Edges

First Approach. Given a plane graph $G = (S, E)$, we encode the shortest paths in $\widehat{E} = \{\hat{e} : e \in E\}$. This encoding generalizes a result in [7][Theorem 2]. Let $I \subset S \times E'$ be the set of all incident vertex-edge pairs (s, e') in the image graph G. The code for $\widehat{E}$ consists of the following:

- The image graph $G = (S, E')$;
- for every incidence $(s, e') \in I$, the number $\mathrm{inc}(s, e')$ of paths in $\widehat{E}$ that start or end at s and contain edge e';
- for every edge $e' \in E'$, the number $\mathrm{vol}(e')$ of paths in $\widehat{E}$ that contain edge e';

Lemma 9 *The shortest paths in $\widehat{E}$ corresponding to a plane graph $G = (S, E)$ are uniquely determined by $G' = (S, E')$, $\mathrm{inc}(s, e')$ for all incidences $(s, e') \in I$, and $\mathrm{vol}(e')$ for all $e' \in E'$.*

Proof. We show that a routing diagram of $G = (S, E)$ can be reconstructed up to isotopy from $G' = (S, E')$ and the values $\mathrm{vol}(e')$ and $\mathrm{inc}(s, e')$. The number of segments in each corridor N_{st}, for $st \in E$, are given by $\mathrm{vol}(st)$. It is enough to determine the routing diagram in the disks D_s for each vertex $s \in S$ independently

(see Fig. 2(d)). That is, it is enough to determine the multiset of edge pairs (rs, st) that belong to some path in $\widehat{E}$ that traverses vertex s.

Consider a vertex $s \in S$. If s is not pointed in G', then no path in $\widehat{E}$ traverses s by Corollary 6. Assume now that s is pointed in G'. For every edge $e' \in E'$ incident to s, the number of paths in $\widehat{E}$ that contain edge e' and traverse s is exactly $\mathrm{vol}(e') - \mathrm{inc}(s, e')$. The total number of paths traversing s is $\frac{1}{2}\sum_{t \in S}[\mathrm{vol}(st) - \mathrm{inc}(s, st)]$. By Lemma 5, the convex angles of the paths traversing s are nested. Therefore, we can successively match the incident edges of s, starting with the pair of edges of the reflex angle at s in G', and continuing until all available edges are used. □

Corollary 10 *The isotopy class of a plane graph $G = (S, E)$ is determined by the shortest paths $\widehat{E}$.*

Proof. The shortest paths in $\widehat{E}$ determine the image graph $G' = (S, E')$, $\mathrm{inc}(s, e')$ for all incidences $(s, e') \in I$, and $\mathrm{vol}(e')$ for all $e' \in E'$. By Lemma 9, these determine a routing diagram up to isotopy. Since there exists a routing diagram isotopic to G [11], $\widehat{E}$ determines the isotopy class of G. □

The above encoding, however, may require a superlinear number of bits. A plane graph with $O(n)$ 1-bend edges can produce homotopic shortest paths of $\Theta(n^2)$ total length [9]. In this case, the average volume of an edge $e' \in E'$ is $\Theta(n)$, and the binary encoding of $\mathrm{vol}(e')$ requires $\Theta(\log n)$ bits. For all edges $e' \in E'$, this code requires $\Theta(n \log n)$ bits. Consequently, this encoding yields a trivial upper bound of $b_1(n) = 2^{O(n \log n)}$. In the next approach, we show how to use $O(n \log(2 + k))$ bits to encode the geodesics $\widehat{E}$ for k-bend edges.

Second Approach: Minimum-Turn Paths. We decompose the homotopic shortest paths in $\widehat{E}$ into subpaths that can easily be reconstructed with a greedy strategy. Instead of recording $\mathrm{vol}(e')$ for every edge $e' \in E'$, we record the first and last edges of these subpaths, and reconstruct $\mathrm{vol}(e')$ from this information.

A directed path $(s_1, s_2, \ldots, s_m)$ in a plane straight-line graph $G' = (S, E')$ is a *min-left-turn* path if all interior vertices are pointed in G', and for $i = 2, \ldots, m-1$ the angle $\angle(s_{i-1}, s_i, s_{i+1})$ is minimal among all angles $\angle(s_{i-1}, s_i, s)$ where $s_i s \in E'$. Analogously, it is a *min-right-turn* path if all interior vertices are pointed in G', and angle $\angle(s_{i+1}, s_i, s_{i-1})$ is minimal among all angles $\angle(s, s_i, s_{i-1})$ where $s_i s \in E'$. A *min-turn* path is a directed path that is either a min-left-turn or a min-right-turn path. Note that a min-left-turn (resp., min-right-turn) path $(s_1, s_2, \ldots, s_m)$ is uniquely determined by its first edge $s_1 s_2$ and its last vertex s_m: each edge of the path determines the next.

We now encode the geodesic shortest paths $\widehat{E} = \{\hat{e} : e \in E\}$ using min-turn paths. Assume that the image graph $G' = (V, E')$ is connected, otherwise we encode the paths in each component of G' separately. Decompose each path $\hat{e}$ into the minimum number of min-turn paths (note that $\hat{e}$ is an undirected path, and it may be decomposed into min-turn paths of opposite directions). Some of the min-turn paths may pass through the leftmost point $s_0 \in S$; decompose these min-turn paths further into two min-turn paths: one ending and one starting at s_0. Denote by P_1 and P_2 the set of resulting min-left-turn and min-right-turn paths, respectively. The new code for $\widehat{E}$ consists of the following:

- The image graph $G = (S, E')$;
- for every incidence $(s, e') \in I$ and $j \in \{1, 2\}$
  - the number $\mathrm{inc}(s, e')$ of paths in $\widehat{E}$ that start or end at s and contain edge e';
  - the number $\mathrm{start}_j(s, e')$ of paths in P_j that start at s and contain edge e'; and
- for every $s \in S$ and $j \in \{1, 2\}$, the number $\mathrm{end}_j(s)$ of paths in P_j that end at s.

Lemma 11 *The shortest paths in $\widehat{E}$ corresponding to a plane graph $G = (S, E)$ are uniquely determined by $G' = (S, E')$, and the quantities $\mathrm{inc}(s, e')$, $\mathrm{start}_j(s, e')$, and $\mathrm{end}_j(s)$ for all $(s, e') \in I$, $s \in S$, and $j \in \{1, 2\}$.*

Proof. By Lemma 9, it is enough to determine the number $\mathrm{vol}(e')$ of shortest paths that contain edge e' for every edge $e \in E'$. Every edge $st \in E'$ is the first edge of $\mathrm{start}_j(s, st)$ min-turn-paths in P_j, for $j \in \{1, 2\}$. For $j = 1, 2$ and $e' \in E'$, let $\mathrm{vol}_j(e')$ denote the number of paths in P_j in which e' is an edge. Then $\mathrm{vol}(e') = \mathrm{vol}_1(e') + \mathrm{vol}_2(e')$, and it suffices to determine the values $\mathrm{vol}_j(e')$ for $j \in \{1, 2\}$.

Assume $j = 1$ (the case $j = 2$ is analogous). If $st \in E'$ is an interior edge of a min-left-turn path in P_1, then s is a pointed vertex in G' and st is the second leg in counterclockwise order of the reflex angle of s. Furthermore, s is not the left-most vertex $s_0 \in S$ (by construction, s_0 is not the interior vertex of any path in P_1). Let F' be the subgraph of G' on the vertex set S that contains, for every pointed vertex $s \in S$, $s \neq s_0$, the second leg of the reflex angle at s. Observe that F' is a forest. Indeed, assume to the contrary that F' contains a cycle $(s_1, \ldots, s_\ell)$. Then for every $i \leq \ell$, vertex s_i is pointed in G' and w.l.o.g. edge $s_i s_{i+1}$ is the second leg of the reflex angle of s_i. Consequently all edges in G' incident to s_i lie in the closed halfplane on the left of $\overrightarrow{s_i s_{+1}}$. Since G' is connected, $(s_1, \ldots, s_\ell)$ is a counterclockwise cycle on the boundary of the convex hull of S. The leftmost vertex $s_0 \in S$ is on the boundary of the convex hull, but the second leg of its reflex angle is not part of the graph F'. The contradiction confirms our claim that F' is a forest.

We define a flow network N_j, for $j \in \{1, 2\}$ as follows: It contains the forest F' with undirected edges and unbounded capacities; two new nodes, a source a and a sink b; and for every vertex $s \in S$, a directed edge as of capacity $\sum_{e':(s,e')\in I} \mathrm{start}_j(s, e')$ and a directed edge sb of capacity $\mathrm{end}_j(s)$. It is clear that the union of min-left-turn paths forms a maximum flow from a to b, since these paths saturate the edges leaving a and the edges entering b. The network has a unique maximum flow since all nonsaturated edges are in F', hence they cannot form a cycle. Consequently, the network N_j determines the the values $\mathrm{vol}_j(e')$ for all $e' \in E'$ and $j \in \{1, 2\}$. □

Lemma 12 *If the shortest paths in $\widehat{E}$ corresponding to a plane graph $G = (S, E)$ can be decomposed into a total of L min-turn paths, then $\widehat{E}$ can be encoded using $O(n \log(2 + L/n))$ bits.*

Proof. The number of plane straight-line graphs $G' = (S, E')$ on n points is $O(187.53^n)$ [32]. Consequently, each planar straight-line graph on S can be encoded using $O(n)$ bits.

Since the image graph is connected and planar, the number of incident vertex-edge pairs $|I|$ in G' is bounded by $|I| = 2|E'| \geq 2(n-1)$ from below and $|I| = 2|E'| \leq 6n$ from above. The number of endpoints of shortest paths in $\widehat{E}$ is $\sum_{(s,e')\in I} \mathrm{inc}(s, e') = 2|\widehat{E}| = 2|E| \leq 6n$. After splitting the min-turn paths at the leftmost point $s_0 \in S$, if necessary, we have at most $2L$ min-turn paths in P, hence $\sum_{(s,e')\in I} \mathrm{start}_j(s, e') \leq 2L$ and $\sum_{s\in S} \mathrm{end}_j(s) \leq 2L$ for $j \in \{1, 2\}$. The integers $\mathrm{inc}(s, e')$, $\mathrm{start}_j(s, e')$, and $\mathrm{end}_j(s)$ can be encoded by $O(\log(2 + \mathrm{inc}(s, e')))$, $O(\log(2 + \mathrm{start}(s, e')))$, and $O(\log(2 + \mathrm{end}(s)))$ bits, respectively. By Jensen's inequality, the numbers $\mathrm{inc}(s, e')$ have binary representation of size

$$\begin{aligned}\sum_{(s,e')\in I} O(\log(2 + \mathrm{inc}(s, e'))) &\leq O\left(|I| \log\left(\frac{\sum_{(s,e')\in I}(2 + \mathrm{inc}(s, e'))}{|I|}\right)\right)\\ &\leq O\left(6n \log\left(\frac{12n + 6n}{2n - 2}\right)\right) = O(n).\end{aligned}$$

The numbers $\mathrm{start}_j(s, e')$ have binary representation of size

$$\begin{aligned}\sum_{(s,e')\in I} O(\log(2 + \mathrm{start}_j(s, e'))) &\leq O\left(|I| \log\left(\frac{\sum_{(s,e')\in I}(2 + \mathrm{start}_j(s, e'))}{|I|}\right)\right)\\ &\leq O\left(6n \log\left(\frac{12n + 2L}{2n - 2}\right)\right) = O(n \log(2 + L/n)),\end{aligned}$$

and analogously $\sum_{s\in S} O(\log(2+\mathrm{end}_j(s))) \le O(n\log(2+L/n))$ for $j\in\{1,2\}$. Overall, our code uses $O(n\log(2+L/n))$ bits. □

In Sections 3.1 and 3.2, we show that a shortest path homotopic to a k-bend edge can be decomposed into $O(k)$ min-turn paths.

3.1 Plane Graphs with 1-Bend Edges

In this section, we show that the geodesic shortest path of a 1-bend edge can be decomposed into at most two min-turn paths: at most one min-left-turn path and at most one min-right-turn path. A polygonal path $(s_1,\dots,s_m)$ is *convex* if it lies on the boundary of the convex hull of the point set $\{s_1,\dots,s_m\}$.

Lemma 13 *If $G=(S,E)$ is a plane graph with 1-bend edges, then every $\hat{e}\in\widehat{E}$ is a convex path.*

Proof. Let $e=(s_1,p,s_m)$ be a 1-bend edge between s_1 and s_m. Consider the points $S_{1,m}=S\cap \mathrm{ch}(s_1,p,s_m)$ lying in the convex hull of s_1, p, and s_m (Fig. 4). If $S_{1,m}=\{s_1,s_m\}$, then the homotopic shortest path is $\hat{e}=s_1s_m$. Otherwise $\hat{e}$ is part of the boundary of $\mathrm{ch}(S_{1,m})$ between s_1 and s_m in the interior of $\mathrm{ch}(s_1,p,s_m)$. In both cases, e can be deformed into $\hat{e}$ within the triangle $\mathrm{ch}(s_1,p,s_m)$. □

Note that for every 1-bend edge $e\in E$, the union of e and $\hat{e}$ forms a *pseudo-triangle* $e\cup\hat{e}$: a simple polygon whose convex vertices are the two endpoints of e and the bend point of e. See Fig. 4 for examples. Since e and $\hat{e}$ are homotopic, no point of S lies in the interior of the pseudo-triangle $e\cup\hat{e}$.

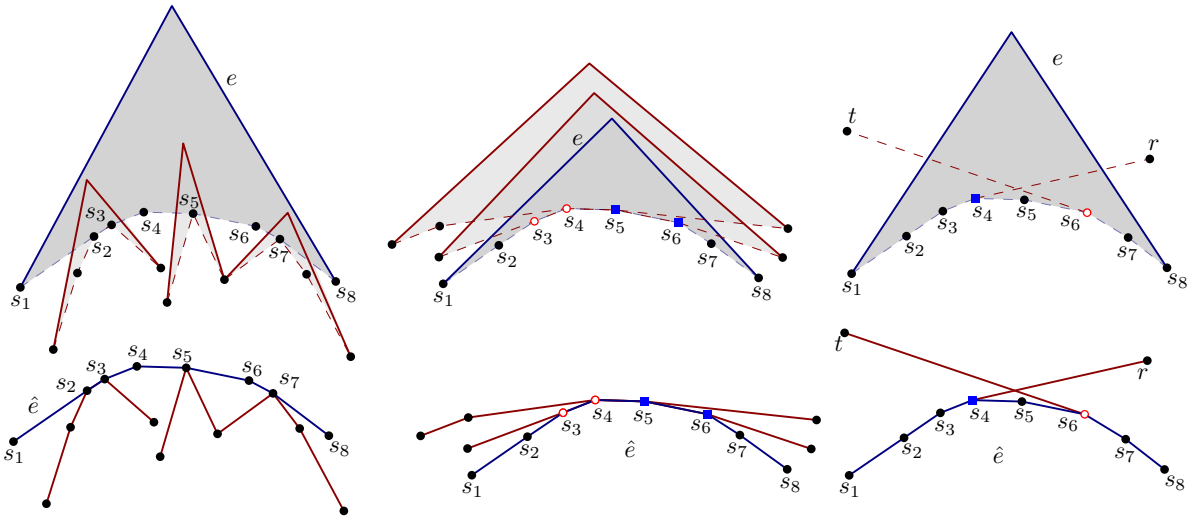

Figure 4: Three examples in two views: solid one-bend edges and dashed homotopic shortest paths (top); and solid homotopic shortest paths (bottom). Left: A shortest path $\hat{e}$ intersects several pairwise disjoint paths. Middle: A shortest path $\hat{e}$ overlaps with several intersecting paths. Right: If s_4 is blue (square) and s_6 is red (circle) in $\hat{e}=(s_1,\dots,s_8)$, then the edges s_4r and ts_6 would cross in G'.

We use the convention that $\hat{e}=(s_1,\dots s_m)$ is labeled such that the angles $\angle(s_{i-1},s_i,s_{i+1})$ are convex (and the angles $\angle(s_{i+1},s_i,s_{i-1})$ are reflex). By Lemma 5, the interior vertices $s_2,\dots,s_{m-1}$ of $\hat{e}$ are pointed in G'. However, the reflex angles $\angle(s_{i+1},s_i,s_{i-1})$ are not necessarily the same as the reflex angles of the graph G' (e.g., angles at red and blue vertices in Fig. 4). Consider a path $\hat{e}=(s_1,\dots,s_m)$ in G'. We say that an interior vertex s_i, $1<i<m$, is

- *red* in $\hat{e}$ if $s_{i-1}s_i$ is not on the boundary of the reflex angle of G' at s_i (i.e., $s_{i-1}s_i$ is not one of the sides of the reflex angle; e.g., s_3 and s_4 in Fig. 4, middle);

- *blue* in $\hat{e}$ if $s_i s_{i+1}$ is not adjacent to the reflex angle of G' at s_i (e.g., s_5 and s_6 in Fig. 4, middle);
- *regular* in $\hat{e}$ if both $s_{i-1}s_i$ and $s_i s_{i+1}$ are adjacent to the reflex angle of G' at s_i.

The key observation for the efficient encoding of the paths in $\widehat{E}$ is that the red and blue vertices can be (weakly) separated in every $\hat{e} \in \widehat{E}$.

Lemma 14 *Let $G = (V, E)$ be a 1-bend plane graph. Then every path $\hat{e} = (s_1, \ldots, s_m)$ can be decomposed into two paths: one is incident to s_1 and its interior vertices are not blue; and the other is incident to s_m and its interior vertices are not red (the common endpoint of the two paths may be both red and blue).*

Proof. Suppose to the contrary that $\hat{e} = (s_1, \ldots, s_m)$ has two interior vertices, s_i and s_j with $1 < i < j < m$, such that s_i is blue and s_j is red. Refer to Fig. 4, right. Recall that s_i and s_j are pointed in G' by Lemma 5. Denote by $r \in S$ and $t \in S$ the two points such that the reflex angles of G' at s_i and s_j, respectively, are $\angle(r, s_i, s_{i-1})$ and $\angle(s_{j+1}, s_j, t)$. By Lemma 5, $s_{i-1}s_i$ and $s_i r$ belong to a shortest path $\hat{e}_1$ for some $e_1 \in E$. Similarly, ts_j and $s_j s_{j+1}$ belong to a shortest path $\hat{e}_2$ for some $e_2 \in E$. Both r and t lie in the exterior of the pseudo-triangle $e \cup \hat{e}$, since $r, t \in S$. Therefore, the segments $s_i r$ and ts_j cross in the interior of $e \cup \hat{e}$. This contradicts the fact that G' is a plane straight-line graph. □

Lemma 14 readily provides a decomposition of each $\hat{e}$ into two min-turn paths.

Corollary 15 *Let $G = (S, E)$ be a 1-bend plane graph. Then every $\hat{e} \in \widehat{E}$ is the union of up to two min-turn paths starting from the endpoints of e.*

Proof. Consider the decomposition of $\hat{e} = (s_1, \ldots, s_m)$ into two paths as in Lemma 14, and direct them such that they start from s_1 and s_m, respectively. Since every interior vertex of the path starting from s_1 (resp., s_m) is red or regular (resp., blue or regular), it is a min-turn path. □

Corollary 15 combined with Lemmata 11 and 12 implies that the number of 1-bend plane graphs on a set S of n points in the plane is $2^{O(n)}$. This confirms Theorem 1 for $k = 1$.

3.2 Extension to k-Bend Edges – Proof of Theorems 1 and 2

In this section, we show that the geodesic shortest path of a k-bend edge can be decomposed into at most $2k$ min-turn paths. The strategy for 1-bend edges in Subsection 3.1 generalizes to k-bend edges: the main difference is that $e \cup \hat{e}$ need not be a simple polygon. By Lemma 8, there is a sequence of $X = (x_1, \ldots, x_\ell)$ intersection points in $e \cap \hat{e}$ such that $x_1 = s_1$, $x_\ell = s_m$, there is a point x_i on each inflection edge of $\hat{e}$, and the corresponding subarcs of e and $\hat{e}$ between x_i and x_{i+1} are interior-disjoint and homotopic for $i = 1, \ldots, \ell - 1$ (see Fig. 5). The corresponding subarcs of e and $\hat{e}$ (with common endpoints) bound simple polygons P_i, $i = 1, \ldots, \ell - 1$, whose interior contains no points from S.

Suppose that $(x_1, s_2, s_3, \ldots, s_{m-1}, x_m)$ is a subarc of $\hat{e}$, where the endpoints are $x_1, x_m \in e \cap \hat{e}$ are consecutive points in X. Since every inflection edge of $\hat{e}$ is subdivided, all angles $\angle(s_{i-1}, s_i, s_{i+1})$ are convex for $i = 2, \ldots, m - 1$, or they are all reflex. Assume they are all reflex (the case of convex angles is analogous). We can distinguish *red*, *blue*, and *regular* interior vertices in the same way as in the case of 1-bend edges. We generalize Lemma 14 as follows.

Lemma 16 *Let $G = (V, E)$ be a plane graph with polyline edges. Let $(x_1, s_2, \ldots, s_{m-1}, x_m)$ be a subarc of $\hat{e} \in \widehat{E}$ such that the corresponding subarc of e has $\ell \geq 1$ bends. Then this subarc cannot contain a subsequence $(s_{\sigma(1)}, \ldots, s_{\sigma(2\ell)})$ such that $1 < \sigma(1) < \ldots < \sigma(2\ell) < m$, and $s_{\sigma(j)}$ is red when j is even and blue when j is odd.*

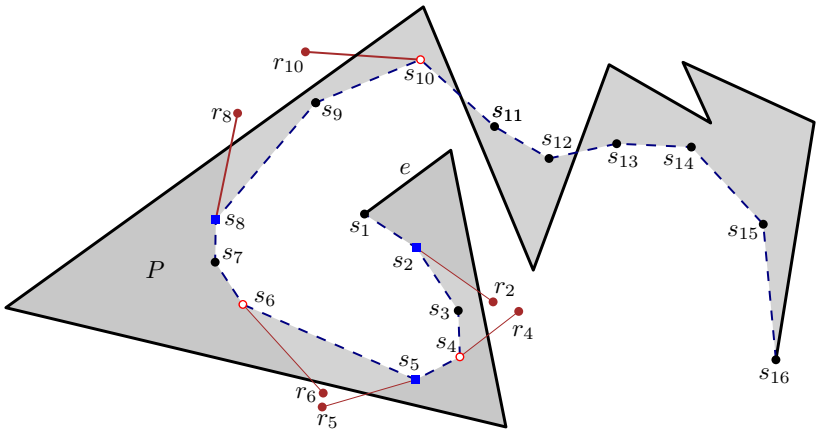

Figure 5: An edge $e = s_1 s_{16}$ with $k = 9$ bends, and its homotopic shortest path $\hat{e} = (s_1, \ldots, s_{16})$.

Proof. Suppose to the contrary that $\hat{\gamma} = (x_1, s_2, \ldots, s_{m-1}, x_m)$ contains a subsequence $(s_{\sigma(1)}, \ldots, s_{\sigma(2\ell)})$ of length 2ℓ such that $s_{\sigma(j)}$ is red when j is even and blue when j is odd. Refer to Fig. 5. For the red vertices $s_{\sigma(j)}$, j even, there is a vertex $r_{\sigma(j)} \in S$ such that the reflex angle of G' at $s_{\sigma(j)}$ is $\angle(s_{\sigma(j)+1}, s_{\sigma(j)}, r_{\sigma(j)})$. Similarly, for the blue vertices $s_{\sigma(j)}$, j odd, there is a vertex $r_{\sigma(j)} \in S$ such that the reflex angle of G' at $s_{\sigma(j)}$ is $\angle(r_{\sigma(j)}, s_{\sigma(j)}, s_{\sigma(j)-1})$. The segments $s_{\sigma(j)} r_{\sigma(j)}$, $j = 2, \ldots, m-1$, are pairwise noncrossing since they are edges of the image graph G'.

Let P be the simple polygon bounded by $\hat{\gamma}$ and the corresponding subarc of e. The points $r_{\sigma(j)}$ for $j = 2, \ldots, m-1$ lie in the exterior of P. Hence the segments $s_{\sigma(j)} r_{\sigma(j)}$ decompose the interior of polygon P into $2\ell + 1$ simply connected *regions*. We now argue that every other region is bounded by a reflex arc and a portion of the edge e: hence the portion of e on its boundary must include a bend point. It follows that the number of bend points is at least $\ell + 1$, contradicting our assumption that the relevant subarc of e has only ℓ bends. Indeed, the path $(x_1, s_2, \ldots, s_{\sigma(1)}, r_{\sigma(1)})$ is reflex by construction. Similarly, the path $(r_{\sigma(2\ell)}, s_{\sigma(2\ell)}, s_{\sigma(2\ell)+1}, \ldots, s_{m-1}, x_m)$ is reflex. For every even index $j < 2\ell$, the path $(r_{\sigma(j)}, s_{\sigma(j)}, \ldots, s_{\sigma(j+1)}, r_{\sigma(j+1)})$ is also reflex. □

Corollary 17 *Let e be a polyline edge with k bends in G. Then every $\hat{e}$ can be decomposed into at most $2k$ min-turn paths.*

Proof. The intersection points in $e \cap \hat{e}$ decompose e and $\hat{e}$ into at most k subarcs such that each subarc of e contains at least one bendpoint. Suppose that e is decomposed into $p \leq k$ subarcs with $\ell_1, \ldots, \ell_p$ bends. By Lemma 16, the ith subarc of $\hat{e}$ can be decomposed into at most $2\ell_i$ paths such that every interior vertex of a path is either (red or regular) or (blue or regular). These paths are min-turn paths with the appropriate orientation. The total number of min-turn paths is at most $\sum_{i=1}^{p} 2\ell_i = 2k$, as claimed. □

Proof of Theorem 1. Let S be a set of n points in the plane. Each planar graph in $B_k(S)$ can be embedded as a plane graph $G = (S, E)$ with k-bend edges. The total number of bends is at most $K \leq (3n)k = 3kn$. The edges in E are in one-to-one correspondence with the homotopic shortest paths in $\widehat{E} = \{\hat{e} : e \in E\}$. The paths in $\widehat{E}$ can be decomposed into at most $2K$ min-turn paths (Corollary 17), and consequently encoded using $O(n \log(2 + K/n)) = O(n \log(2 + k))$ bits, as claimed. □

Proof of Theorem 2. Let S be a set of n points in the plane. Each isotopy class in $T_k(S)$ is represented by a plane graph $G = (S, E)$ with polyline edges and at most K bends. Each isotopy class uniquely determines a set of homotopic shortest paths $\widehat{E} = \{\hat{e} : e \in E\}$ (Corollary 10), which can be decomposed into at most $2K$ min-turn paths (Corollary 17), and consequently encoded with $O(n \log(2 + K/n))$ bits (Lemma 12). □

4 Triangulations with Polyline Edges

In this section, we consider augmenting the graphs in $B_k(S)$ with new edges. In Section 4.1, we consider adding a new k-bend edge to a given embedding of a cycle, and note an interesting dichotomy based on the parity of k. In Section 4.2, we present the main result of this section; we show that an edge-maximal graph in $B_k(S)$ need not be a combinatorial triangulation. We construct a point set $S \subset \mathbb{R}^2$ and a graph $G \in B_k(S)$ such that no matter how G is embedded on S with k bends per edge, it cannot be augmented into a combinatorial triangulation.

4.1 Embedded cycles with k-bends per edge

For triangulating a single face in a k-bend embedding of an n-vertex cycle C_n, we observe a dichotomy based on the parity of k.

Proposition 18 *Let k and n be integers with $k \geq 1$ and $n \geq 3$.*

1. *If k is odd, then there is a k-bend embedding of C_n in which the inner (resp., outer) face cannot be triangulated using k-bend edges.*
2. *If k is even, then in every k-bend embedding of the cycle C_n the inner and the outer face can each be triangulated using k-bend edges.*

Note that the second statement does not extend to the case $k = 0$: the outer face of a geometric triangulation on a vertex set S is the complement of the convex hull $\mathrm{ch}(S)$, which might not be a triangle.

We use the concept of visibility and link distance [26] in our argument for odd k. Let a k-bend embedding of a graph G be given. We say that two points p and q are mutually *visible* if the line segment pq is interior-disjoint from (the embedding of) the edges of G. Two vertices v_1 and v_2 can be connected by a 1-bend edge in a face F if both v_1 and v_2 see a point (the bend point) in F. The set of points in F visible from a point v is the *visibility region* of v in F.

Similarly, v_1 and v_2 can be connected by a k-bend edge in face F, for k odd, if and only if there is a point $p \in F$ that can be connected to both v_1 and v_2 with $\lfloor k/2 \rfloor$-bend polylines, or equivalently, there is a point $p \in F$ with link distance to both v_1 and v_2 at most $\lceil k/2 \rceil$.

In the proof of Proposition 18, we shall use Sperner's Lemma [34], a well-known discrete analogue of Brouwer's fixed point theorem.

Lemma 19 (Sperner [34]) *Let K be a geometric simplicial complex in the plane, where the union of faces is homeomorphic to a disk. Assume that each vertex is assigned a color from the set $\{1, 2, 3\}$ such that three vertices $v_1, v_2, v_3 \in \partial K$ are colored 1, 2, and 3, respectively, and for any pair $i, j \in \{1, 2, 3\}$, the vertices on the path between v_i and v_j along ∂K that does not contain the 3rd vertex are colored with $\{i, j\}$. Then K contains a triangle whose vertices have all three different colors.*

Proof of Proposition 18 We prove statements 1 and 2 separately.

Odd k. For $k = 1$, consider the embedding of the cycle C_4 in Fig. 6(a). Any two nonadjacent vertices have disjoint visibility regions in the inner face F, consequently no two nonadjacent vertices can be connected by a 1-bend edge in F. Similarly, in the embedding of the cycle C_4 in Fig. 7(a), any two nonadjacent vertices have disjoint visibility regions in the outer face F, consequently the outer face cannot be triangulated.

Both constructions generalize for all odd $k \in \mathbb{N}$. For the inner face F, we modify the polygon in Fig. 6(a) by replacing each segment incident to a vertex with a zigzag path with $\lfloor k/2 \rfloor$ bends as indicated in Fig. 6(b-c). As a result, the sets of points in F at link distance at most $\lceil k/2 \rceil$ from two nonadjacent vertices are disjoint.

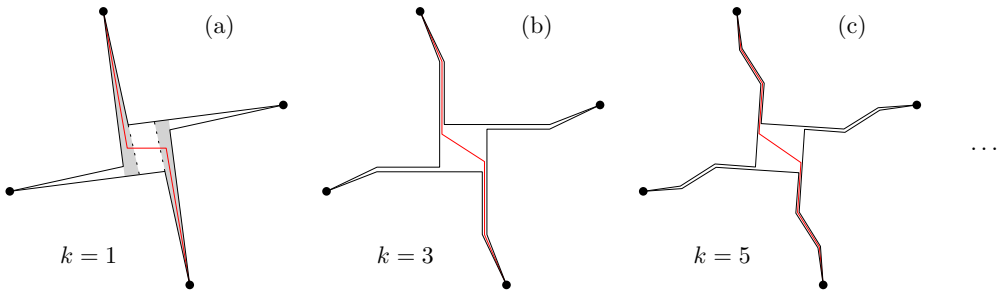

Figure 6: A plane realization of C_4 with k-bend edges, for $k = 1, 3, 5$, such that the interior of C_4 cannot be subdivided into two triangles by a single k-bend diagonal.

When F is the outer face, we modify the polygon in Fig. 7(a) by replacing each segment incident to a vertex with a spiral that winds around the convex hull with $\lfloor k/2 \rfloor$ bends as in Fig. 7(b-c). Here again, the sets of points in F at link distance at most $\lceil k/2 \rceil$ from two nonadjacent vertices will be disjoint.

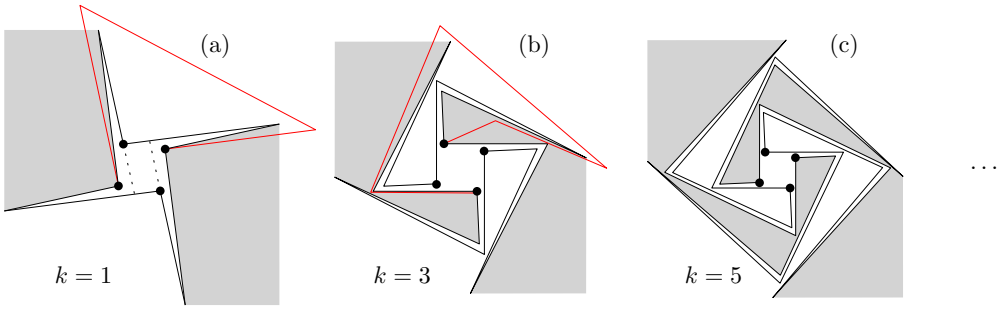

Figure 7: A plane realization of C_4 with k-bend edges, for $k = 1, 3, 5$, such that the exterior of C_4 cannot be subdivided into two triangles by a single k-bend diagonal.

Even k. Let $k \geq 2$ be an even integer. We proceed by induction on n. The claim trivially holds for $n = 3$. Assume that $n \geq 4$ and that the claim holds for all cycles with fewer than n vertices. It is enough to show that in every k-bend embedding of C_n, the inner and the outer face can each be subdivided by a new k-bend edge between two nonadjacent vertices. Then each subface can be triangulated by induction.

Let S be a set of $n \geq 4$ points in the plane, and consider a cycle $C_n = (S, E)$ with a k-bend embedding. Assume, by perturbing the points if necessary, that the union of S and all bend points is in general position (no three collinear points), and every edge has precisely k bends. Let F be the inner or outer face of C_n.

Subdivide each edge with k new vertices placed at the bend points: we obtain a straight-line embedding of a cycle $C_{n(k+1)} = (S', E')$, which is a simple polygon with $n(k + 1)$ vertices in general position. We introduce a 3-coloring of S' as follows: let $S = \{s_i : i = 1, \ldots, n\}$. Assign color 1 to the vertex s_1; color 2 to vertex s_i if i is even, and color 3 to vertex s_i if is odd and $i \geq 3$. For each vertex s_i, assign the color of s_i to the $k/2$ closest bend points along the cycle. (Note that this is not a proper coloring.) Construct an arbitrary geometric triangulation T of F; and let $K(T)$ denote the simplicial complex formed by the bounded triangles in T. See Fig. 8(a)-(b) for an example. We distinguish two cases.

Case 1: F is the inner face. In this case, the simplicial complex $K(T)$ is homeomorphic to a disk. By Sperner's Lemma [34], T contains a 3-colored triangle. Let (a, b, c) be a 3-colored triangle in T. Vertex a (resp, b and c) lies in a $(k/2)$-neighborhood of some vertex in S along the cycle $C_{n(k+1)}$. Since $n \geq 4$, at least one pair of vertices in $\{a, b, c\}$ is in the $(k/2)$-neighborhoods of two nonadjacent vertices of C_n. Without loss of generality, ab is such an edge where a and b lie in the $k/2$-neighborhoods of s_i and s_j,

respectively, where $j \notin \{i-1, i, i+1 \mod n\}$. We can now construct a polyline p with at most k bends between s_i and s_j along the edges of T: Concatenate the polyline from s_i to a along C_k, the edge ab, and the polyline from b to s_j along C_k. Perturb the interior vertices of p by moving them into the interior of F along the angle bisectors of the incident edges (Fig. 8(c)). We obtain a k-bend edge between s_i and s_j that lies in F.

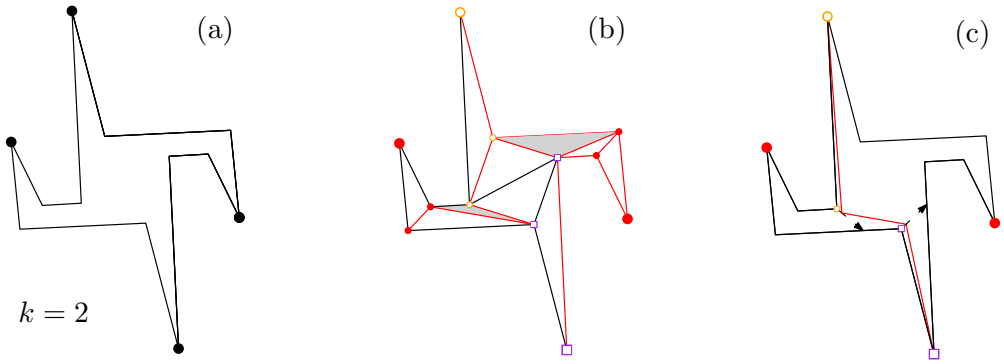

Figure 8: (a) A 2-bend embedding of C_4. (b) The coloring of the vertices and bend points, and a triangulation of the inner face. Two properly colored triangles are highlighted. (c) The triangulation contains a polyline with $k = 2$ bends between two opposite vertices; which can be perturbed into a 2-bend edge lying in the inner face.

Case 2: F is the outer face. In this case $K(T)$ is homotopy equivalent to a circle (the hole corresponds to the inner face of C_n), and the argument in Case 1 does not go through in general. The outer face of T is the complement of $\mathrm{ch}(S')$. Each vertex of $\mathrm{ch}(S')$ is incident to both the inner face of $C_{n(k+1)}$ and the outer face of T. Consequently, the vertices of $\mathrm{ch}(S')$ decompose $K(T)$ into components, each of which is either a single edge or homeomorphic to a disk. If any of these components contain 3 or more vertices from S, the argument of Case 1 produces a desired new k-bend edge. Suppose that all these components contain 2 or fewer vertices from S. Note that for each vertex $s_i \in S$, there is a polyline p_i with at most $k/2$ edges (i.e., $k/2 - 1$ bends) to a vertex incident to $\mathrm{ch}(S')$. Consider two arbitrary nonadjacent vertices of C_n, say s_i and s_j. Extend the last edges of the polylines p_i and p_j to some points a and b, respectively, in the exterior of $\mathrm{ch}(S')$. We may assume that the last edges of p_i and p_j are nonparallel. If a and b are sufficiently far from $\mathrm{ch}(S')$, then the line segment ab lies in the outer face F. The concatenation of p_i, ab, and p_j gives a polyline with at most k bends between s_i and s_j. A perturbation described in Case 1 yields a k-bend edge between s_i and s_j that lies in F. □

Remark. Proposition 18(2) does not generalize to all embedded graphs with k-bend edges when k is even. Figure 9 shows two graphs embedded with 2-bend edges that cannot be triangulated: the addition of the 2-bend diagonals in the shaded faces would introduce double edges.

4.2 Combinatorial triangulations realizable with k-bend edges

For a graph in $G = (S, E)$ in $B_k(S)$, $k \geq 1$, the vertex set is fixed, but bend points can vary. If one embedding cannot be triangulated with k-bend edges, another embedding with different bend points may still be. In this section we show that an edge-maximal graph in $B_1(S)$ may have arbitrarily many and arbitrarily large bounded faces.

Theorem 3 *For every $f, h \in \mathbb{N}$, with $f \geq 4$ and $h \geq 1$, there is a point set S and a graph $G = (S, E)$ such that G is an edge-maximal graph in $B_1(S)$ and every 1-bend plane embedding of G has at least h bounded faces each with f edges.*

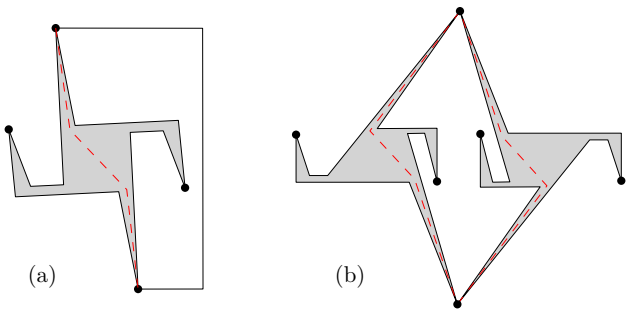

Figure 9: Two graphs embedded with 2-bend edges that cannot be triangulated.

Proof. We present the proof for $f = 4$ and $h = 1$. The proof for larger values of f are analogous, and extensions to larger values of h follow from repeating congruent copies of S and isomorphic copies of G.

Consider the (labeled) graph G on 20 vertices in Figure 10(a). It contains a 4-cycle $(1, 2, 3, 4)$, each edge of which is adjacent to a separating triangle around the points 9, 10, 11, and 12, respectively; and it also contains an 8-cycle $(1', \ldots, 8')$ around the first 12 vertices.

We construct a labeled point set S. We have $S = A \cup B$ where $A = \{1, \ldots, 12\}$ and $B = \{1' \ldots, 8'\}$. The points in A are arranged as in Fig. 10(c). The cycle $(1, 2, 3, 4)$ forms a square; it contains a smaller square $(9, 10, 11, 12)$ such that $W = (1, 9, 2, 10, 3, 11, 4, 12)$ forms a windmill-shaped polygon (see Fig. 10(c)), that is, the visibility ranges of vertices 1 and 3 (resp., 2 and 4) are disjoint in the interior of W. Points $5, \ldots, 8$ are sufficiently close to $1, \ldots, 4$, respectively, such that any substitution in W between corresponding pairs of close vertices maintains a windmill-shaped polygon. The points in B are the vertices of a regular octagon $(1', \ldots, 8')$ such that (i) it is concentric with $(1, 2, 3, 4)$ and (ii) its diameter is 4 times larger than the diameter of A. Figure 10(b-c) show a 1-bend embedding of G on S, confirming that $G \in B_1(S)$.

Since G is planar and 3-connected, it has a unique combinatorial embedding [36] (up to the choice of the outer face). We show that in every 1-bend embedding of G on S, the face $F = (1, 2, 3, 4)$ cannot be triangulated. Suppose, to the contrary, that G admits a 1-bend embedding in which F can be triangulated. By the rotational symmetry of the construction, we may assume that edge $\{2, 4\}$ triangulates F. That is, there is a bend point x visible to both 2 and 4 in F. We next derive conditions on the possible location of x.

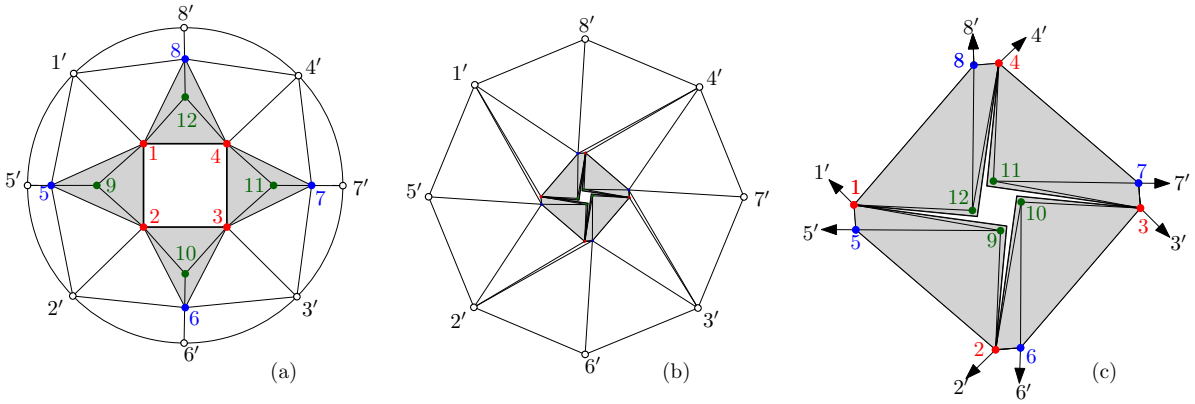

Figure 10: (a) Graph G, with four shaded separating triangles. (b) A 1-bend embedding of G on the point set S where face $(1, 2, 3, 4)$ cannot be triangulated; see subfigure (c) for a detailed view of vertices $1, ..., 12$. (c) The point set A and the embedding of its induced subgraph.

We first argue that all faces of the embedding that are induced by A are bounded. Specifically, we claim that for every integer $t \geq 3$, the interior of a t-cycle induced by A contains at most t points from B. Let C_t

be such a cycle, and suppose its interior contains $b' \in B$. Since B is disjoint from $\mathrm{ch}(A)$, point b' lies in the convex hull of a 1-bend edge of C_t, say $\{u, v\}$. The convex hull of edge $\{u, v\}$ is a triangle (u, v, w), where w is the bend point. Since $u, v \in A$, the triangle (u, v, w) is contained in a slab of width at most $\mathrm{diam}(A)$. However, every such slab contains zero, one, or two opposite points from B. Consequently, at most one point of B lies in the interior of (u, v, w), and at most t points in the interior of C_t, as claimed. It follows that $(1, 2, 3, 4)$ can contain at most 4 out of 8 points of B, and so it is a bounded face. Similarly, the interiors of the separating triangles $(1, 2, 5)$, $(2, 3, 6)$, $(3, 4, 7)$, and $(4, 1, 8)$ each contain three bounded faces induced by A, as well as the points 9, 10, 11, and 12, respectively.

Consider the separating triangle $(1, 2, 5)$. Point 9 lies in the interior of $(1, 2, 5)$, but not in $\mathrm{ch}(1, 2, 5)$. Therefore, 9 lies in the convex hull of one of the 1-bend edges $\{1, 2\}$, $\{2, 5\}$, or $\{1, 5\}$. If the convex hull of $\{1, 2\}$ or $\{2, 5\}$ contains 9, then the segment of the edge incident to vertex 2 is to the right of $\overrightarrow{(2, 9)}$, hence the bend point $x \in F$ lies in the right halfplane of $\overrightarrow{(2, 9)}$. If the convex hull of $\{1, 5\}$ contains 9, then x is either in the right halfplane of $\overrightarrow{(2, 9)}$ as in the previous case, or in the left halfplane of $\overrightarrow{(2, 9)}$ but in the right halfplane of $\overrightarrow{(1, 9)}$. In the latter case, however, the line segment $x4$ crosses the convex hull of the 1-bend edge $\{1, 5\}$, and so this case can be ruled out. Therefore, in all cases, x lies in the halfplane on the right of $\overrightarrow{(2, 9)}$.

An analogous argument for separating triangle $(3, 4, 7)$ and point 11 implies that x lies in the right halfplane determined by $\overrightarrow{(4, 11)}$. By construction of the point set A, the two halfplanes that contain x are disjoint. We conclude that there is no point x visible from both 2 and 4. □

For all even $k \geq 2$, Proposition 18(2) implies the following.

Proposition 20 *Let $k \geq 2$ be an even integer, and $S \subset \mathbb{R}^2$ a finite point set in general position. Then every 3-connected edge-maximal graph in $B_k(S)$ is a combinatorial triangulation.*

Proof. Suppose, to the contrary, that there is a 3-connected graph $G = (S, E)$ that is edge-maximal in $B_k(S)$ but not a combinatorial triangulation. Consider an arbitrary k-bend embedding of G. Since G is not a combinatorial triangulation, the embedding contains some face F bounded by 4 or more edges. By Proposition 18(2), face F has two nonadjacent vertices, say u and v, that can be connected by a new k-bend edge in F. The edge $\{u, v\}$ is not present in E, otherwise $\{u, v\}$ would be a 2-cut in G. Consequently, G can be augmented to a strictly larger graph in $B_k(S)$, contradicting its maximality. □

Remark. The 3-connectivity condition was crucial in the proof of Proposition 20. It is possible that a 2-connected edge-maximal graph in $B_2(S)$ is not a combinatorial triangulation. For example, the 2-bend embedding in Fig. 9(b) has two quadrilateral faces, but it cannot be augmented to a combinatorial triangulation in $B_2(S)$, since the only possible 2-bend diagonals of the two quadrilaterals are parallel edges.

It is likely that Theorem 3 generalizes to all odd integers $k \geq 1$, by ensuring that every k-bend embedding has a face with a certain shape, as in Fig. 6. We do not pursue generalizations of Theorem 3 for $k \geq 2$ here.

5 Monotone Embeddings

An embedding of a graph in the plane is called *monotone* if every edge is embedded as an x-monotone Jordan arc. We show that the number of n-vertex labeled graphs that admit a monotone embedding on a given set of n points in the plane is super-exponential.

Theorem 4 *For every set S of n points in the plane, no two on a vertical line, at least $\lfloor (n-2)/2 \rfloor !$ labeled planar graphs with $n \geq 4$ vertices admit a monotone embedding on S.*

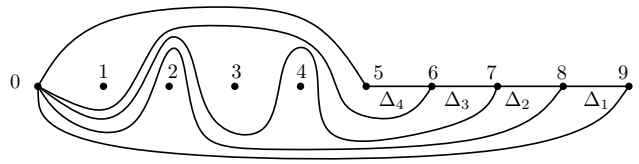

Figure 11: A monotone plane graph on the vertex set $S = \{0, 1, \ldots, 9\}$ corresponding to the permutation given by $\pi(2) = 1$, $\pi(2) = 4$, $\pi(3) = 3$, and $\pi(4) = 1$.

Proof. We may assume w.l.o.g. that n is even, and let $n = 2m + 2$ for some $m \in \mathbb{N}$. We may also assume that the vertices are integer points on the x-axis $S = \{(i, 0) : i = 0, \ldots, 2m + 1\}$ by applying a homeomorphism that preserves x-monotonicity. We label the vertices by their x-coordinates $i = 0, 1, \ldots, 2m + 1$. We construct a family of $m!$ nonisomorphic planar graphs on n vertices, together with suitable plane embeddings on the point set S using x-monotone edges.

The leftmost vertex is 0. Partition the remaining $2m + 1$ vertices into two sets: $A = \{1, \ldots, m\}$ and $B = \{m + 1, \ldots, 2m + 1\}$. In all graphs that we construct, the vertices in B are joined by a path $(m + 1, \ldots, 2m + 1)$, and vertex 0 is adjacent to all vertices in B. For $i = 1, 2, \ldots, m$, the triangle $\Delta_i = (0, 2m + 2 - i, 2m + 1 - i)$ is induced by 0 and two vertices in B. Each Δ_i will contain exactly one vertex $\pi(i) \in A$; and $\pi(i)$ is adjacent to the three corners of the triangle Δ_i. By construction, $\pi : [m] \to [m]$ is a permutation. Note that any two permutations correspond to nonisomorphic labeled graphs.

We show that every permutation $\pi : [m] \to [m]$ produces a graph that admits a monotone embedding on S. For a given permutation $\pi : [m] \to [m]$, a monotone embedding can be constructed as follows. The edges of the path $(m + 1, \ldots, 2m + 1)$ are realized by horizontal straight-line segments. For every edge $e_i = (0, 2m + 1 - i)$, $i = 0, 2, \ldots, m$, we incrementally construct an x-monotone path: Let edge e_0 be a monotone path below the x-axis. When e_i has been constructed, then draw e_{i+1} such that it closely follows e_i from above, but makes a loop above vertex $\pi(i) \in A$. See Fig. 11 for an example. Finally, connect each point $i \in A$ to the three corners of Δ_i with three monotone paths.

The $m!$ permutations $\pi : [m] \to [m]$ produce $m!$ pairwise nonisomorphic labeled planar graphs, each of which admits a monotone embedding onto the labeled point set S. □

6 Conclusions

Theorem 1 bridges the gap between the number $2^{\Theta(n)}$ of straight-line graphs and the number $2^{\Theta(n \log n)}$ of graphs embedded with $k = 120n$ bends per edge on a set of n points in the plane. Our upper bound $b_k(n) \leq 2^{O(n \log(2+k))}$ on the number of graphs that embed on n points in the plane with k-bend edges is the best possible, apart from the hidden constants, for all $k, n \in \mathbb{N}$, $0 \leq k \leq 120n$. We have introduced the graph class $B_k(S)$ for every finite point set $S \subset \mathbb{R}^2$ and integer $k \geq 0$. It is a natural question whether the graphs in these classes can be recognized efficiently. For $k = 0$ and $n = |S|$, an $O(n \log n)$-time algorithm can decide whether a graph $G = (S, E)$ is in $B_0(S)$, by simply testing intersections between nonadjacent edges (line segments). For $k = 1$, the problem is already NP-hard. Bastert and Fekete [5] proved that, given a point set S and a graph $G = (S, E)$, it is NP-hard to decide whether G admits a 1-bend embedding. Similarly, we can ask whether a graph $G = (S, E)$ is in $B_k(S)$, for $k \geq 2$; or approximate the minimum integer k such that $G = (S, E)$ is in $B_k(S)$. Finding the minimum k such that $G = (S, E)$ admits a k-bend embedding, or minimizing the *total number* of bends are already known to be NP-hard [5].

We do not know what the minimum bit complexity of a 1-bend embedding is when the vertices have integer coordinates. Specifically, if S is a subset of an $m \times m$ section of the integer grid in $\mathbb{R}^2$, what is the minimum refinement of the grid that can accommodate all bend points in some embedding of any graph in $B_1(S)$? A related algorithmic question concerns finding homotopic paths with geometric constraints:

Polynomial-time algorithms are known [6, 11, 12] for finding homotopic shortest paths for pairwise non-crossing polyline edges; but no efficient algorithm is known for finding homotopic shortest 1-bend edges for a given 1-bend embedding of a graph in $B_1(S)$.

In Section 4, we have seen that for some point sets S there exists graphs $G \in B_k(S)$ that cannot be triangulated in $B_k(S)$ when $k = 1$. We believe that there exist similar instances for every odd integer $k \geq 1$, but analysing all possible k-bend embeddings of a graph $G \in B_k(S)$ requires additional tools when $k \geq 3$. We do not know of any combinatorial characterization of graphs $G \in B_k(S)$ that can be triangulated, or whether such graphs can be recognized efficiently.

Acknowledgements. Work on this problem started at the *11th Gremo Workshop on Open Problems* (Sellamatt, SG, Switzerland, 2013). We thank all participants of the workshop for the stimulating environment.

References

[1] O. Aichholzer, T. Hackl, B. Vogtenhuber, C. Huemer, F. Hurtado, and H. Krasser, On the number of plane geometric graphs, *Graphs and Combinatorics* **23(1)** (2007), 67–84.

[2] M. Ajtai, V. Chvátal, M. Newborn, and E. Szemerédi, Crossing-free subgraphs, *Annals Discrete Math.* **12** (1982), 9–12.

[3] V. Alvarez, K. Bringmann, R. Curticapean, and S. Ray, Counting crossing-free structures, *Comput. Geom. Theory. Appl.* **48(5)** (2015), 386–397

[4] P. Angelini, G. Da Lozzo, G. Di Battista, V. Di Donato, P. Kindermann, G. Rote, and I. Rutter, Windrose planarity: embedding graphs with direction-constrained edges, in *Proc. 27th Symposium on Discrete Algorithms*, SIAM, 2016, pp. 985–996.

[5] O. Bastert and S. P. Fekete, Geometric wire routing, Technical Report 332, University of Cologne, 1998.

[6] S. Bespamyatnikh, Computing homotopic shortest paths in the plane, *J. Algorithms* **49(2)** (2003), 284–303.

[7] S. Bespamyatnikh, Encoding homotopy of paths in the plane, in *Proc. 6th LATIN*, LNCS 2976, Springer, 2004, pp. 329–338.

[8] N. Bonichon, C. Gavoille, N. Hanusse, D. Poulalhon, and G. Schaeffer, Planar graphs, via well-orderly maps and trees, *Graphs and Combinatorics* **22(2)** (2006), 185–202.

[9] S. Cabello, Y. Liu, A. Mantler, and J. Snoeyink, Testing homotopy for paths in the plane, *Discrete Comput. Geom.* **31(1)** (2004), 61–81.

[10] H.-C. Chang, J. Erickson, and C. Xu, Detecting weakly simple polygons, in *Proc. 26th Symposium on Discrete Algorithms*, SIAM, 2015, pp. 1655–1670.

[11] É. Colin de Verdière, Shortening of curves and decomposition of surfaces, Ph.D. thesis, Université Paris 7, 2003.

[12] É. Colin de Verdière and J. Erickson, Tightening nonsimple paths and cycles on surfaces, *SIAM J. Comput.* **39(8)** (2010), 3784–3813.

[13] É. Colin de Verdière, Computational Topology of graphs on surfaces, chapter 23 in *Handbook of Discrete and Computational Geometry*, 3rd edition, CRC Press, to appear.

[14] É. Colin de Verdière and F. Lazarus, Optimal system of loops on an orientable surface, *Discrete Comput. Geom.* **33(3)** (2005), 507–534.

[15] P. F. Cortese, G. Di Battista, M. Patrignani, and M. Pizzonia, On embedding a cycle in a plane graph, *Discrete Mathematics* **309** (7) (2009), 1856–1869.

[16] A. Dumitrescu, A. Schulz, A. Sheffer, and Cs. D. Tóth, Bounds on the maximum multiplicity of some common geometric graphs, *SIAM J. Discrete Math.* **27(2)** (2013), 802–826.

[17] C. A. Duncan, A. Efrat, S. Kobourov, and C. Wenk, Drawing with fat edges, *Intern. J. Found. Comput. Sci.* **17** (2006), 1143–1164.

[18] A. Efrat, S. G. Kobourov, and A. Lubiw, Computing homotopic shortest paths efficiently, *Comput. Geom. Theory Appl.* **35** (2006), 162–172.

[19] J. Erickson and K. Whittlesey, Transforming curves on surfaces redux, in *Proc. 24th Symposium on Discrete Algorithms*, SIAM. 2013, pp. 1646–1655.

[20] H. Everett, S. Lazard, G. Liotta, and S. K. Wismath, Universal sets of n points for one-bend drawings of planar graphs with n vertices, *Discrete Comput. Geom.* **43(2)** (2010), 272–288.

[21] O. Giménez and M. Noy, Asymptotic enumeration and limit laws of planar graphs, *J. AMS* **22** (2009), 309–329.

[22] J. Hershberger and J. Snoeyink, Computing minimum length paths of a given homotopy class, *Comput. Geom. Theory Appl.* **4(2)** (1994), 63–97.

[23] P. Hoffman and B. Richter, Embedding graphs in surfaces, *J. Combin. Theory Ser. B* **36(1)** (1984), 65–84.

[24] M. Hoffmann, M. Sharir, A. Schulz, A. Sheffer, Cs. D. Tóth, and E. Welzl, Counting plane graphs: flippability and its applications, in *Thirty Essays on Geometric Graph Theory (J. Pach, ed.)*, Springer, 2013, pp. 303–326.

[25] M. Kaufmann and R. Wiese, Embedding vertices at points: few bends suffice for planar graphs, *J. Graph Algorithms Appl.* **6(1)** (2002), 115–129.

[26] A. Maheshwari, J.-R. Sack, and H. N. Djidjev, Link distance problems, in *Handbook of Computational Geometry (J. Sack and J. Urrutia, eds.)*, chap. 12, 1999, Elsevier, pp. 517-558.

[27] P. Minc, Embedding of simplicial arcs into the plane, *Topology Proceedings*, **22** (1997), 305–340.

[28] J. Pach and G. Tóth, Monotone drawings of planar graphs, *J. Graph Theory* **46(1)** (2004), 39–47. See also `arXiv:1101.0967v1`.

[29] J. Pach and R. Wenger, Embedding planar graphs at fixed vertex locations, *Graphs and Combinatorics* **17(4)** (2001), 717–728.

[30] F. Santos and R. Seidel, A better upper bound on the number of triangulations of a planar point set, *J. Combin. Theory Ser. A* **102** (2003), 186–193.

[31] M. Sharir and A. Sheffer, Counting triangulations of planar point sets, *Electronic J. Combinatorics* **18** (2011), P70.

[32] M. Sharir and A. Sheffer, Counting plane graphs: cross-graph charging schemes, *Combinat. Probab. Comput.* **22** (2013), 935–954.

[33] M. Sharir and E. Welzl, Random triangulations of planar point sets, in *Proc. 22nd ACM Sympos. on Comput. Geom.*, ACM Press, 2006, pp. 273–281.

[34] E. Sperner, Neuer Beweis für die Invarianz der Dimensionszahl und des Gebietes, *Abh. Math. Sem. Hamburg* **6** (1928), 265–272.

[35] G. Turán, On the succinct representation of graphs, *Discrete Appl. Math.* **8** (1984), 289–294.

[36] H. Whitney, Congruent Graphs and the Connectivity of Graphs, *Amer. J. Math.* **54** (1932), 150–168.